

We are IntechOpen, the world's leading publisher of Open Access books Built by scientists, for scientists

6,900

Open access books available

186,000

International authors and editors

200M

Downloads

Our authors are among the

154

Countries delivered to

TOP 1%

most cited scientists

12.2%

Contributors from top 500 universities



WEB OF SCIENCE™

Selection of our books indexed in the Book Citation Index
in Web of Science™ Core Collection (BKCI)

Interested in publishing with us?
Contact book.department@intechopen.com

Numbers displayed above are based on latest data collected.
For more information visit www.intechopen.com



Wastewater Treatment through Low Cost Adsorption Technologies

Gonzalo Montes-Atenas and Fernando Valenzuela

Additional information is available at the end of the chapter

<http://dx.doi.org/10.5772/67097>

Abstract

This chapter addresses the wastewater treatment of mining residues through adsorption methodologies. It preferentially focuses its attention on (but not limited to) the removal of heavy metals. It begins with a brief description of the most used wastewater treatment pathways highlighting both their advantages and disadvantages and focusing on adsorption industrial practice. Classic models of adsorption thermodynamics and kinetics are presented. It finalises with a more detailed description of two methodologies of low cost sorbents: (i) inorganic nanostructured silicates and (ii) organic-based sorbents—pine bark.

Keywords: adsorption, adsorbent, wastewater treatment, sorbent, mathematical modelling, mining

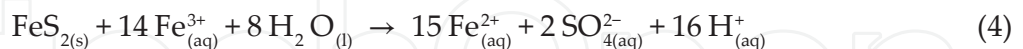
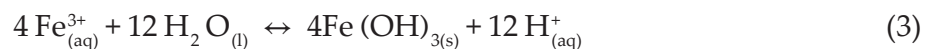
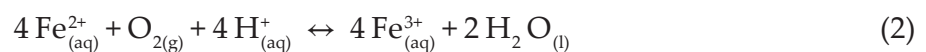
1. Wastewaters containing heavy metals and other contaminants: mining applications

1.1. Introduction

One of the two major environmental problems concerning the management of liquids in mining and mining-related activities, particularly relevant to a country like Chile, is the natural generation of acidic mine drainages (AMD) or acidic rock drainages (ARD) produced by chemical and/or microbial oxidation of sulphides in the presence of air and water [1, 2]. Obviously, the other problem is the impact of industrial residual aqueous solutions originated in the metallurgical and mining processing plants. All these solutions exhibit an important amount of chemical contaminants, either dissolved or suspended, at concentrations that normally surpass the limit fixed by the national discharge regulations and their

discard in an acceptable manner into surface and groundwater bodies is an imperious need [3]. The complexity behind the latter issue is even higher considering that the water requirements in the mining industry are becoming a real problem, especially in regions such as the Atacama Desert or The Andes Mountains, where this vital liquid is scarce. Mining activities must then share the few water resources with the needs of the local communities for human life and agriculture. Therefore, it is absolutely necessary to optimise the use of all the available water resources, by controlling the waters entering mining and metallurgical plants and by treating the liquid residues that the processes such as leaching, solvent extraction and froth flotation plants produce.

For instance, AMD occurs when sulphide ores, mainly iron- and copper-bearing sulphides minerals, are exposed to water and air, resulting in the formation of sulphuric acid and metal hydroxides that release toxic heavy metal ions, and acidic hydrogen into surface and ground waters [4, 5]. They are also generated at waste disposal sites and around abandoned mine sites. Its formation is primarily a function of the local geology and hydrology. The AMD usually consists of an aqueous solution that exhibits a variable acidity and contains many and variable toxic or valuable dissolved metals, with a high content of sulphate (SO_4^{2-}) and other anions such as phosphate (PO_4^{3-}), nitrate (NO_3^-), molybdate (MoO_3^{2-}) and chloride (Cl^-), and a high amount of colloidal-type suspended fine solids difficult to settle, becoming a water pollution problem difficult to remediate. The metals remain in solution until the pH increases to a level where precipitation occurs. However, precipitation presents many problems, such as redissolving of precipitates, the need of a large amount of chemicals and the generation of large volumes of sludge whose disposal is quite complex. Just as an exemplification, some chemical reactions that represent the chemistry of AMD formation are as follows [6, 7]:



Equation (1) represents the oxidation of pyrite by oxygen. This reaction generates two moles of acid per mole of oxidised pyrite. Reaction (2) involves the conversion of Fe(II) into Fe(III), reaction that is enhanced by the bacteria *Acidithiobacillus ferrooxidans* (whenever these microorganisms are present in the system). Reaction (3) represents the hydrolysis of iron with the formation of the corresponding hydroxide and the production of new acid molecules. Finally, reaction (4) represents the oxidation of additional pyrite by ferric iron generated in the previous reactions. These reactions are based on the dissolution of pyrite (FeS_2); nevertheless, it is expected that they also occur simultaneously with other metal sulphides present in the ore. An overall chemical reaction cycle takes place very rapidly and continues until either the ferric iron or the metal sulphide is depleted. The latter implies that a variety of metals and anions may dissolve in the process both conferring a significant toxicity to the streams containing them and turning AMD into a potential source of many valuable and, sometimes, scarce metals.

1.2. Wastewater treatment paths and their comparison to adsorption operations

Solubility driven treatments: Precipitation operations widely used in the removal of heavy metals are implemented based on pH or the addition of counter-ions leading the formation of sparingly soluble compounds (Eqs. (5) and (6), respectively)



In these cases, the solubility product constants and the solubility of the compounds are written as in Eqs. (7) and (8).

$$K_{ps} = a_{M^{n+}} a_{OH^-}^n \quad s = \sqrt[n+1]{\frac{K_{ps}}{n}} \quad (7)$$

$$K_{ps} = a_{X^{m-}}^m a_{M^{n+}}^n \quad s = \sqrt[m+n]{\frac{K_{ps}}{m+n}} \quad (8)$$

where K_{ps} and a_i represent the solubility product constant and the activity or real (effective) concentration of the ion i in the aqueous solution.

The remaining amount of the pollutant in the solution depends on the species solubility which is not only a function of the solubility product constant but also of the number and equilibrium constants associated with the formation of anionic and others species related to counterions forming other molecular complexes [8]. The formation of metal hydroxides may leave large amounts of pollutants in aqueous solutions. In this case, counterions with lower K_{ps} values are used, for instance sulphide ions (S^{2-}) are used to improve the wastewater treatment of waters containing mercury or cadmium. Most of the treatments employed in our country only consider a alkaline chemical treatment by contacting the acidic stream with $CaCO_3$ or CaO or $Ca(OH)_2$ raising the pH up to a point where metals are partially precipitated.

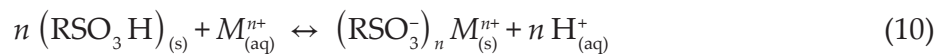
Cementation and other electrochemically driven treatments: Cementation operations correspond to spontaneous electrochemical reactions largely displaced towards the formation of the products. They have identical problems to those found in classic precipitation operations and, additionally, the process have to deal with the release of the reduction agent (R) to the aqueous phase (Eq. (9)).



Cementation processes are commonly implemented in acidic conditions to avoid metal hydrolysis and consider oxidation reactions which are located outside the water stability domain. The latter introduces in these systems parallel competitive reactions associated with the hydrogen evolution and others decreasing the efficiency of the cementation process. Other non-spontaneous electrochemical treatment is used such as electrodeposition, a clean technology claimed to avoid the generation of residues or electrocoagulation. The latter having an anode made of a polyvalent metal able to promote coagulation such as iron or aluminium. However, according to the elements to be removed, appropriate aqueous solution conditions must be reached. Relatively high cost associated with the application of voltage differences and mass transport limitations due to low conductivity and/or low element concentration make this wastewater treatment strategy expensive compared to other spontaneous processes.

Membrane-based separation treatments: This path includes ultrafiltration, nanofiltration and reverse osmosis. Ultrafiltration allows the removal of dissolved and colloidal materials. Isolated metal ions are difficult to remove directly due to their small sizes so the use of micelles and other complexing agents enhances its separation capabilities. Reverse osmosis removes a wide range of dissolved species from aqueous solutions; however, it has high power pumping requirements to restore the membranes. Membrane separation techniques have gone through significant progresses developing liquid membrane processes based on the formation of emulsions; however, there is still room for improvement with regard to their instability in salty and acidic conditions and fouling produced by other species present in the wastewater. Electrodialysis does not require the addition of external species to the wastewater, exhibits high selectivity and does not produce sludges, which makes it a promising technology. However, energy consumption and anodic/cationic membrane fouling is still a challenge.

Ion-exchange treatment: Ion-exchange resins either natural or synthetic are selected when high treatment capacity, high efficiency and fast kinetics are required. The stronger resins are built on sulphonic or carboxylic groups as in Eqs. (10) and (11). In both cases, the acidification of the aqueous media is commonly observed as it occurs in the case of solvent extraction using kerosene and implemented in countercurrent when using oximes. The only difference between ion exchange and solvent extraction would be that the organic phase would be in the dissolved phase in the organic phase rather than in the solid phase.



Froth flotation: This process can be used to treat wastewaters contaminated with heavy metals and can be implemented following different technologies such as dissolved air flotation (DAF), electroflotation, ion flotation or precipitation flotation. DAF processes are based on the gas oversaturation and decompression producing microbubbles that are able to separate small particles or agglomerates. The electroflotation process is associated with the water electrolysis producing the smallest bubble sizes of hydrogen and oxygen known at the industrial level. Ion flotation is based on ionic complex formation with surfactant molecules and subsequent frother-aided flotation. The precipitation flotation is a mixed technology between the precipitation followed by flotation operations (sulphide precipitation are commonly implemented).

Adsorption separation treatments: In heterogeneous systems, whenever two immiscible states of the matter, namely gas and liquid, gas and solid or liquid and solid, are set in contact they are separated by a surface layer having properties different to those of the two states forming it [9]. When one or more components present in one of the two phases (or in both) tend towards increasing its concentration in the surface layer, it is said that the adsorption process is taking place (**Figure 1**).

In **Figure 1**, the adsorbat is represented by the orange circles. The adsorbent is represented by the continuous marble-like colour. The adsorption process can be either physical or chemical in nature. The physical adsorption or physisorption requires energies in the order of some kcal/mol and is mainly associated with condensation processes of the species at the interface. Its spontaneity is enhanced by reducing the temperature of the system (Eq. (12)).

$$dG_{\text{ads}} = dH_{\text{ads}} - TdS_{\text{ads}} \quad (12)$$

where dG_{ads} , dH_{ads} , dS_{ads} represent the adsorption Gibbs free energy, the adsorption enthalpy and the adsorption entropy, respectively, while T is the temperature of the system. The term $dH_{\text{ads}} < 0$ (heat of condensation). In consequence, the spontaneity $dG_{\text{ads}} < 0$ would be favoured by lower temperature conditions. In this case, the rate of the adsorption process is rapid, reversible between the adsorbed and desorbed states, and it can be either mono-molecular or multimolecular with respect to the number of adsorbat molecules associated

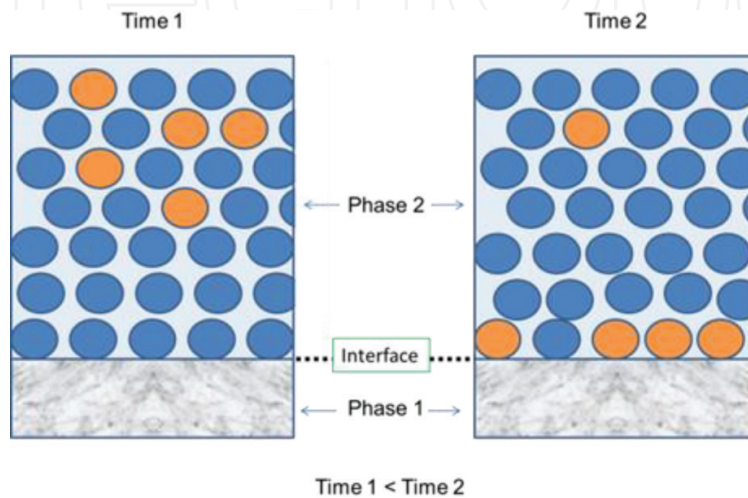


Figure 1. Schematics of an adsorption process.

with the number of available adsorption sites. On the other hand, chemical adsorption or chemisorption requires energies in the order of dozens of kcal/mol and involves the generation of bonding between the adsorbed specie and the interface. In general terms, its spontaneity is enhanced by increasing the temperature as $dH_{\text{ads}} > 0$ (activation energy needs to be reached). The adsorption process is slower and is highly dependent on the adsorbent nature and generally irreversible due to the strong forces between the adsorbat and the adsorbent taking place in the adsorption process. Adsorption operations have grown as a feasible way to treat wastewaters. The process is versatile in terms of the materials that can be used ranging from natural substrates or biosorbents such as stems, bark, leaves, among other; to synthetic sorbents like activated carbon, metal oxides, etc. The maximum adsorption capacity of the sorbent is commonly studied in thermodynamic experiments which are represented in terms of the adsorption isotherms. A list of the most used adsorption isotherms and the systems is presented in **Tables 1** and **2**. The $\frac{V}{V_{\text{max}}}$ ratio represents the adsorbed volume of adsorbat over the maximum volume of adsorbat able to be adsorbed. Otherwise named as a degree of coverage or q/q_{max} where q_i has units of mg of adsorbat/g of sorbent defined as θ . Please, note that q_{max} is referred to as the maximum adsorption associated with the monolayer. In all mathematical expressions, the variable P refers to the pressure of the adsorbat when a gas phase is set in contact with a condensed phase, namely, liquid or solid. In more general terms, the pressure P can be replaced by the activity or concentration of the adsorbat in aqueous phase.

Model No.	Name	Mathematical model	Specific features of the model and when to use it...
(1)	Langmuir [10]	$\theta = \frac{k_1 P}{1 + k_1 P} \quad (3)$ <p>Or</p> $k_1 P = \frac{\theta}{1 - \theta} \quad (3')$ <p>Graphically:</p> $\frac{1}{q_e} = \frac{1}{q_{max}} + \frac{1}{q_{max} k_1 P} \quad (3.5)$ $\frac{P}{q_e} = \frac{1}{k_1 q_{max}} + \frac{P}{q_{max}} \quad (3.6)$ $q_e = q_{max} - \frac{q_e}{k_1 P} \quad (3.7)$ $\frac{q_e}{P} = k_1 q_{max} - k_1 q_e \quad (3.8)$ $\frac{1}{P} = \frac{k_1 q_{max}}{q_e} - k_1 \quad (3.9)$	<p>This two-parameter model is widely used in cases where ideal localised monolayer is obtained by either chemical or physical adsorption. This is perhaps the most relevant model in the field of adsorption and has been derived from kinetic premises, thermodynamics conceptualisation and also statistically [11] The particular conditions under which the model is valid are as follows:</p> <ol style="list-style-type: none"> (1) Once adsorbed the adsorbate is fixed onto one surface site and there is no migration throughout the sorbent surface (or interface). Therefore, the adsorbent exhibits a limited capacity for adsorption (2) One adsorbate molecule is associated with one surface site (3) The surface energy is identical for every surface site and therefore the same applies to the adsorption energy. In other words, the following equation holds $\Delta G_a = \Delta H_a - T \Delta S_a = cte(3.3)$, where the subscript <i>a</i> refers to the adsorption process (4) A homogeneous surface without lateral interaction and steric hindrance between adsorbed species is required even if they are adsorbed in adjacent sorbent surface sites <p>The strength of intermolecular attractive forces decreases dramatically with the distance to the surface sorbent</p>
(2)	Freundlich (also known by the name Halsey and Taylor) (Freundlich, 1906) [12]	$q_e = k_1 P^{\frac{1}{n}} \quad (11)$ <p>Graphically:</p> $\log q_e = \log k_1 + \frac{1}{n} \log P \quad (11.3)$	<p>This two-parameter isotherm is applicable to chemical and physical adsorption without lateral interactions between adsorbed molecules. It is an empirical two parameter model which describes a multilayer adsorption process where the surface sites do not follow any uniform distribution in adsorption heat of adsorption or affinities between the sorbent and adsorbent. It is based on the fact that the concentration of the adsorbate on the surface increases with the concentration in the other phase</p> <p>The conditions are</p> <ol style="list-style-type: none"> 1. The heat of adsorption can be represented by $-\Delta H_a = -\Delta H_0 \text{Log} \theta$ (11.1). 2. The model cannot be used at high and low degree of coverage. At very low adsorbate concentration, the Freundlich equation does not provide Henry's law; however, it is valid for ion adsorption at low solute concentrations <p>If $\frac{1}{n}$ is close to zero, the surface heterogeneity of the sorbent is more significant. Such heterogeneity is characterised by the exponential decaying sorption site distribution (or the adsorption enthalpy changes logarithmically with the degree of coverage). Particularly, in this case, when <i>n</i> varies from 1 to 10, the adsorption is highly favourable. If <i>n</i> is then, the partition between the two phases is independent of the concentration of the adsorbate and linear adsorption occurs. If $\frac{1}{n}$ is higher than 1, there is a symptom of cooperative adsorption</p>

Model No.	Name	Mathematical model	Specific features of the model and when to use it...
(3)	Redlich-Peterson [13]	$q_e = \frac{k_r P}{1 + a_r P^{\phi}} \quad (24)$ <p>Graphically,</p> $\ln\left(k_r \frac{P}{q_e} - 1\right) = \phi \ln P + \ln a_r$	<p>This is an empirical three parameter isotherm model that can be applied to sorbents exhibiting homogeneous and heterogeneous surface energy within a significant range of pressure or concentration of adsorbate. It is particularly useful for moderate pressures/concentrations. Its use requires evaluating three parameters (k_r, a_r and ϕ) combining aspects from Langmuir and Freundlich isotherms. The denominator consists of a hybrid Langmuir-Freundlich form. The model consists of a linear dependence on the adsorbate concentration/pressure and an exponential behaviour with respect to the same variable in the denominator. At high adsorbate concentration/pressure the model is simplified to the Freundlich isotherm. In any case, if $\phi = 1$ the Langmuir model is obtained. If $\phi = 0$, the Henry's law is obtained</p>

Table 1. Adsorption isotherms and their use.

No	Name	Mathematical model	Meaning of the parameters and when to use it...
(1)	Lagergren Pseudo-first order [14]	<p>Derivative form:</p> $\frac{dq_t}{dt} = k_{kin}(q_e - q_t)$ <p>Integral form:</p> $\ln(q_e - q_t) = \ln q_e - k_{kin} t$	<p>k_{kin} is the specific rate of adsorption q_t is the adsorption parameter which evolves with time. This model is widely used for cases where the adsorbate is originally dissolved in aqueous phase and the adsorption follows a first order equation. The following assumptions are made:</p> <ol style="list-style-type: none"> (1) The adsorption is localised and there is not any interaction between adsorbed molecules (2) The adsorption energy is independent of surface coverage (3) Maximum adsorption capacity is equivalent to the monolayer formation (4) The concentration of the adsorbate in the fluid phase is constant
(2)	Pseudo-second order	<p>Derivative form:</p> $\frac{dq_t}{dt} = k_{kin}(q_e - q_t)^2$ <p>Or,</p> $q_t = q_e \left[1 - \frac{1}{\beta_2 + k_2 t} \right]$ <p>Integral form:</p> $\frac{t}{q_t} = \frac{1}{k_{kin} q_e^2} + \frac{t}{q_e}$	<p>k_{kin} is the specific rate of adsorption This model assumes that the chemisorption is the rate determining step in the process. These assumptions are similar to the pseudo-first order but in this case the adsorption follows a second-order kinetics</p>
(4)	Intra-particle diffusion or Weber and Morris model [15]	$q_t = k_{id} \sqrt{t} + I$	<p>k_{id} intraparticle diffusion rate constant I provides information about thickness of the boundary layer If the plot of q_t vs \sqrt{t} passes through the origin. Otherwise, the overall adsorption mechanism is also controlled (to some degree) by a boundary layer</p>

Table 2. Adsorption kinetics models.

2. Inorganic sorbents case study: Silica based sorbents - Nanostructured silicates

2.1. Introduction

The synthesis, characterisation and performance of sorbents based on nanostructured calcium silicates without modification or chemically modified with other atoms with the purpose to improve the adsorption of some specific contaminant species are reviewed. The nanostructured calcium silicates possess a very high capacity to remove contaminants from water even when these are present in higher concentrations, and also have the capability of a collective and simultaneous removal of cationic and anionic species from acidic aqueous solutions. Effectively, there is a strong need for adsorbent materials that have the capacity for removing simultaneously both anions and cations from industrial and mining solutions. The synthesized nanostructured calcium silicates exhibit a specific surface area, averaging values over 100–400 m²/g, showing a good sorption capacities for removing high contents of different ionic species. The mechanisms governing the sorption process are related to the presence of silanol, calcium and hydroxyl groups in its structure, which would act as binding or nucleation sites on its surface [16]. Recent efforts for modifying nanostructured calcium silicates by introducing in their structures other metals that generate an improved sorbent addressed to enhance the sorption of other species present in solutions like the AMD, by using simple and low-cost processes, have been achieved. The efficiencies accomplished with nanostructured calcium silicates modified with iron, magnesium and aluminium introduced in its structure opens the possibility of tailoring a mix of modified silicates to suit the composition of various wastewaters requiring decontamination treatment. 'The more insoluble is the hydroxide precipitate or the salt formed during the reaction of the calcium silicate with the ionic species to be removed, the more efficient is the sorption process'.

The following modifications have been obtained successfully:

- (a) Nanostructured calcium silicate derivatives containing Fe atoms have been prepared to selectively promote and enhance the adsorption of arsenic species through the formation of highly insoluble and stable double-salt of calcium and iron.
- (b) The introduction of Mg atoms of *n*-calcium silicate by partial substitution by Ca atoms have permitted the preparation of a sorbent material that benefits the removal of phosphate and ammonium ions, frequently found in mining wastewaters, due the formation of a very insoluble calcium-containing double phosphate of Mg and ammonium.
- (c) The partial replacement of Ca atoms in *n*-calcium silicate by Al atoms generates a stronger sorbent that allow and improve the sulphate removal by forming a high insoluble aluminium and calcium double basic salt.
- (d) Nanostructured calcium silicate by forming a composite with magnetite in order to provide to this nanosorbent of magnetic properties and facilitate its separation from the resulting solution.

This monography addresses the base case and these four case studies.

2.2. Experimental procedures – Nanostructured silicate synthesis procedure

The synthesis of nanostructured calcium silicate can be conducted using several routes of preparation. In this study, calcium silicate was synthesized by precipitation as a result of the room temperature chemical reaction between liquid Na_2SiO_3 and $\text{Ca}(\text{OH})_2$ at a pH value of 12.3, following a process in two steps. Firstly, a suspension of $\text{Ca}(\text{OH})_2$ in water is treated with HCl 33% w/w to give a slurry with a pH value of 12–12.5, varying the stirring velocity in a range between 425 and 1000 min^{-1} . Secondly, a sodium silicate solution containing 28.5% w/w SiO_2 is diluted with water resulting in a 0.32% w/w SiO_2 solution. Then, this solution is vigorously mixed with the previously prepared $\text{Ca}(\text{OH})_2$ suspension in a reactor, varying the stirring velocity between 1000 and 6000 min^{-1} , immediately forming a precipitate, nanostructured calcium silicates containing an average value of 35 g SiO_2/kg of formed solid. The formed slurry is aged for 20 min, allowed to settle for 13 h, before the obtained solid is recovered by vacuum filtration. Afterwards, the filter cake is washed with water and ethanol in order to disperse the nanostructured particles and lower the surface tension of the still wet solid. The solid is dried at 383 K for 2 days. Treatment with ethanol is necessary because during the drying of silicate, which presents a high surface area, is generated a great liquid-air interface that causes a high surface tension collapsing the structure of the material reducing its pore volume and surface area. The synthesised calcium silicate is an amorphous substance which does not present a defined chemical structure as is shown in **Figure 2**.

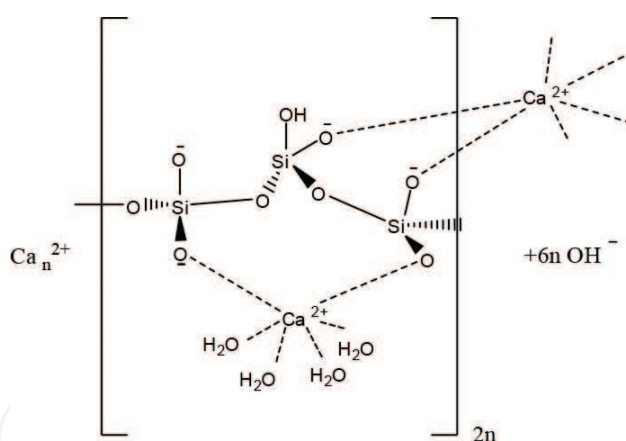


Figure 2. Probable structure of nanostructured calcium silicate.

Figure 2 shows the presence of OH^- groups and adsorbed water on the surface of the material. **Figure 3** shows scanning electron microscope (SEM) micrographs of the synthesised nanostructured calcium silicates. Particles exhibit a mean particle size between 0.2 and 1.0 μm . The particles appear in the SEM pictures forming larger agglomerates. This structure would correspond to a silicate backbone with plates of a thickness around of 10 nm and would consist of a tetrahedral silicate with $\text{Ca}(\text{II})$ ions and silanol groups on the surface forming a wollastonite-like structure, CaSiO_3 , which contains SiO_3^{2-} species in which $\text{Ca}(\text{II})$ ions and the silanol groups would act as probable binding sites for the species being removed. The modifications

done to the adsorbent by introducing other atoms that replace part of the calcium in the silicate, have not change significantly the mentioned structure, making possible the preparation of strong sorbent composites. Because of their low-cost and their disposable character, the regeneration of the modified calcium silicate is not considered. However, given their silicate-base composition similar to cement, later uses can be outlined.

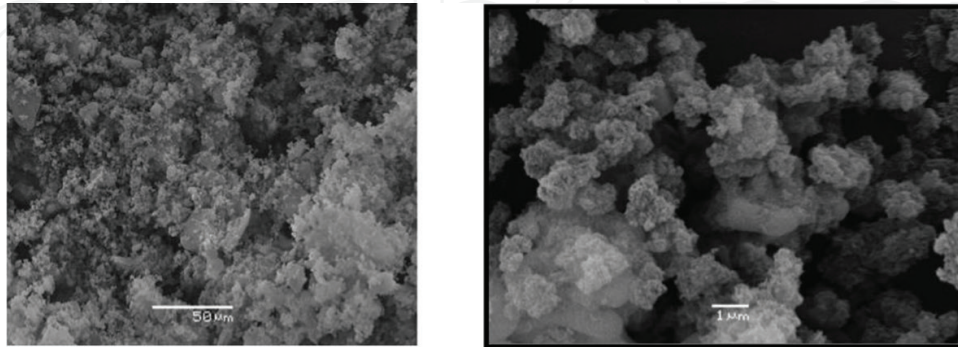


Figure 3. SEM micrographs of the non-modified nanostructured silicate adsorbent.

2.3. Modifications to the nanostructured calcium silicate

Variants of this methodology to generate sorbent modifications are described below:

- (a) Mg -substituted calcium silicate: add Mg during the synthesis of calcium silicate, a variable mole % magnesium is added as $\text{Mg}(\text{OH})_2$ to replace part of the Ca atoms by Mg.
- (b) Fe -calcium silicate: are prepared by replacing part of the calcium atoms of the silicate by Fe atoms using as iron source FeCl_3 or $\text{Fe}(\text{OH})_3$
- (c) Al -substituted calcium silicate, aluminium can be added as NaAlO_2 , $\text{Al}(\text{OH})_3$ or poly-aluminium chloride (PAC) at the start of the synthesis with the $\text{Ca}(\text{OH})_2$.
- (d) Magnetic properties of the calcium silicate that allows its easy separation from the treated waters, during the synthesis are added a suitable proportion of magnetite (Fe_3O_4), what avoid an important degrading of the accessible surface area of the silicate.

In all cases, there is a maximum element to calcium replacement ratio without compromising the nanostructure of silicate. Over certain replacement proportions, the nanostructure suffers a deleterious effect.

2.4. Characterization of nanostructured calcium silicate

The characterisation consisted of:

- Observing by scanning electron microscopy (SEM) JEOL JSM-25SII instrument.
- Measuring the mean particle size using a Malvern Mastersizer Hydro 2000 MU apparatus.

- Carrying out porosimetry analyses including the determination of the specific surface area are conducted using a N_2 sorptometer in a Micromeritics ASAP 2010 porosimeter at 20°C and 1 atm.
- Determining whether the nanostructured calcium silicates present a crystalline or amorphous structure, samples of the prepared solids were analysed using a Bruker D8 advance X-ray powder diffractometer which poses a LynxEye lineal detector.
- Determining the presence of free water molecules, O-H groups associated with water and silanol groups and Si-O bonds, infrared spectra were obtained in a Bruker-FTIR IFS 55.
- Performing differential scanning calorimetry (DSC) analysis using a DSC Perkin Elmer 6000 equipment to check the presence of water and of silanol groups in the silicate.
- Finding the elemental composition of the adsorbent using X-ray fluorescence spectrometry method and chemical analysis. In addition, the content of Ca and Fe in the adsorbent was also measured by flame atomic absorption analysis using a Perkin Elmer PinAAcle 900F apparatus, technique that was also used to check the chemical stability of the sorbent when contacted with acidic-aqueous solutions; these are necessary tests taking into account the acidic nature of most mine wastewaters.

2.5. Adsorption experiments

Batch equilibrium sorption tests are conducted at 303 K in a batch-type reactor by mixing a variable amount of nanostructured calcium silicate and different volumes of a copper mine aqueous solution having the following main composition:

- (a) Main components: pH: 2–6; SO_4^{2-} : 2–10 g/L; Cu(II): 20–120 mg/L; Fe (Fe(II) + Fe(III)): 120–330 mg/L; Zn(II): 15–120 mg/L; Mg(II): 140–250 mg/L; Ca(II): 250–400 mg/L; Mn(II): 80–140 mg/L; P: 20–130 mg/L (in phosphate).
- (b) Minor and toxic components: Cd(II): 5–20 mg/L; Pb(II): 8–30 mg/L; As: 40–200 mg/L; Cr(VI): 0–20 mg/L; Ni(II): 4–5 mg/L; NO_3^- : 10–30 mg/L; Cl⁻: 20–40 mg/L; MoO_4^{2-} : 2–10 mg/L; TSS: 60–250 mg/L; pH: 2.1–4.6.

Batch experiments are conducted over sufficient time to reach equilibrium conditions. During the experiments, samples of the solution are collected at defined intervals and filtered using a 0.45 μm nitrocellulose Millipore membrane. The latter was performed before measuring the pH value and the concentration of metallic ions by atomic absorption spectrophotometry on a Perkin Elmer PinAAcle 900F instrument. The quantity of metal adsorbed is determined by the difference between the concentrations of metal in the initial aqueous feed phase and that in the raffinate solutions. At the end of the tests, the nanostructured calcium silicates were separated from the resulting aqueous solution by filtration. The SO_4^{2-} ion content is determined using a standard barium sulphate method [17] and PO_4^{3-} ion concentration is measured using the vanadate-molybdate-phosphoric UV-spectroscopy method [18].

2.6. Results

2.6.1. Synthesis and characterization

The chemical reaction between Ca(OH)_2 and Na_2SiO_3 is fast generating a thixotropic precipitate that produces particle agglomeration. The reaction of Ca(II) ions with soluble silicate as Na_2SiO_3 resulted in the precipitation of calcium silicate, an insoluble solid, where Ca(II) appeared to be strongly bound to a silicate backbone. The extent of the reaction and the particle size of the solid formed depend strongly on the pH of the reaction mixture, the proportions and concentration of calcium and silicate ions and the intensity of the stirring employed during the process. Intensive stirring in basic medium produces a quite homogeneous but colloidal and amorphous insoluble calcium silicate. The higher the stirring velocity, the smaller the particle size of the resultant calcium silicate and the larger and more accessible the substrate surface area comprising of micro-pores and meso-pores.

The modification of the adsorbent consists of a first step where Ca(OH)_2 and the source of the replacing elements (Mg(OH)_2 or FeCl_3 or the Al compound) are mixed with the HCl solution. Afterwards, the resulting phase is mixed with the Na_2SiO_3 solution at high-stirring velocity, ideally over 2000 min^{-1} . It is not easy to establish a single stoichiometry of the chemical reaction due to the wide variety of silicate species possible to be formed and to the proportion of hydroxyl and silanol groups that silicates would contain. Even the synthesized calcium silicate as an amorphous substance does not present a defined chemical structure as shown in the scheme of **Figure 1**. Notwithstanding, in all cases, the prepared substrate corresponds effectively to an amorphous material without a defined structure. Particles present a mean particle size averaging $0.5\text{--}1.0 \mu\text{m}$ forming larger agglomerates. Details of nanostructured calcium silicate have been described in former communications by Cairns et al. using ^{29}Si -NMR spectroscopy and X-ray photoelectron spectroscopy (XPS) analysis [19]. They suggest the structure consists of a silicate backbone with plates of thickness around 10 nm. It would comprise silicate tetrahedral sites with Ca(II) ions and silanol groups on the surface forming a wollastonite-like structure, CaSiO_3 , where Ca(II) ions and silanol groups would act as probable binding sites. Cairns et al. propose that the calcium silicate would contain 1.5% of hydroxyl groups meaning that approximately 8% of silicon atoms in the structure are silanol groups allowing metallic ions such as Cu(II) and Zn(II) to form the corresponding hydroxides on the surface of the silicates acting as nucleation sites [20]. Porosimetry analyses using the N_2 sorptometer, indicate a variable surface area ranging between 80 and $300 \text{ m}^2/\text{g}$, a value much higher than the surface area shown by other sorbents [21]. The mean pore diameter varies between 11 and 25 nm and the pore volume between 0.200 and $0.400 \text{ cm}^3/\text{g}$ for calcium silicates varying with the stirring velocity used during the synthesis.

X-ray diffraction analysis confirms that the prepared compounds are basically amorphous or at least polycrystalline. However, elements of patterns associated with wollastonite, CaSiO_3 , and larnyta-syn, Ca_2SiO_4 , were observed confirming the synthesis of a calcium silicate. Although natural silicates are crystalline, like natural wollastonite, the solids prepared in this study appeared amorphous, probably because they were prepared by precipitation from aqueous solutions. Soluble silicates found in solutions comprise silicate ions of different size, most of them polymerized, which are not able to organise themselves in a crystal form resulting in a colloidal solid.

2.6.2. Adsorption experiments

Sorption experiments are carried out to measure the capability of these nanostructured calcium silicates to uptake diverse metallic ions and some anions found in many residual industrial and mining wastewaters. Most of the experiments were conducted using the aqueous solutions whose initial metals concentrations have been described before. However, in order to establish the maximum metal sorption capacity of the nanostructured calcium silicates, some experiments were carried out using a feed-aqueous solution with higher content of metals (up to 5 g/L) (**Figure 4**).

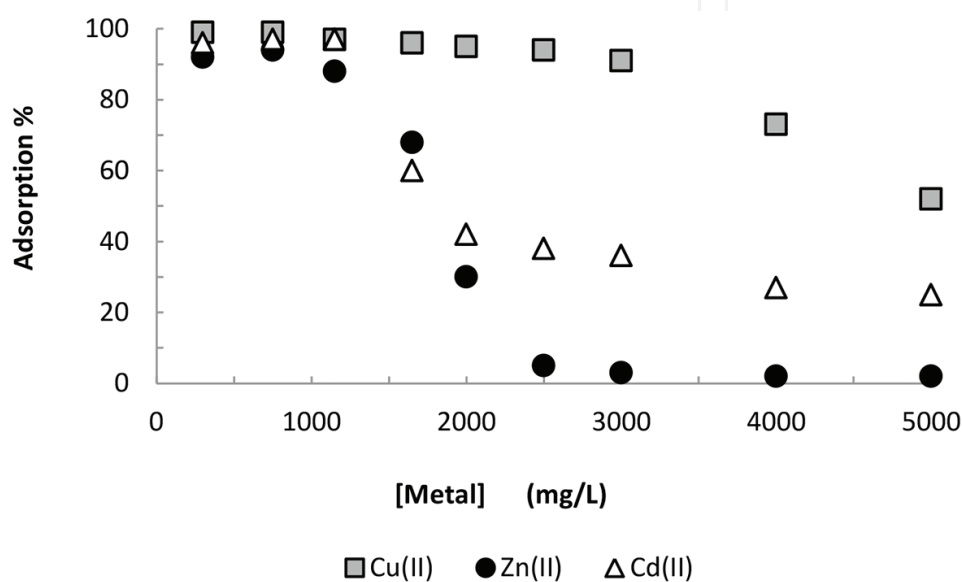


Figure 4. Adsorption of some metallic ions onto nanostructured calcium silicate.

Metallic ions such as Cu(II), Zn(II) and Cd(II) readily form insoluble hydroxides under basic conditions. However, their removal by precipitation only with lime is far from an ideal solution when their content in solution is high enough to consider them pollutants. In the presence of nanostructured calcium silicate the extent of precipitation reached is significantly higher than that observed with only lime being used. The degree of removal of Cu(II), Zn(II) and Cd(II) ions is higher and it produces more stable structures using the nanostructured calcium silicates prepared in this study. In fact, it is reasonable to think that silicates kept the pH value in a more basic region acting as a buffer. Thereby, they ensure a good precipitation of metallic ions probably onto the surface of the formed silicate, rather than in the bulk solution. This way, the precipitates generated in this case are of more granular nature, meaning that they could settle or get filtrated more easily than the precipitates obtained using lime or NaOH. This fact suggested that the metal removal from aqueous solutions would be a cation exchange between the metals to remove and the calcium ions associated with the silicate structure.

Figure 5 presents the results observed for the sorption of the anions PO_4^{3-} , SO_4^{2-} and CrO_4^{2-} introduced in the test solutions employing as a sorbent in the same sample of nanostructured

calcium silicate without modification. The adsorption of PO_4^{3-} is fairly significant, SO_4^{2-} is also adsorbed, until a maximum uptake point. Cr(VI) is not adsorbed at all probably because this ion is present in aqueous solution as anionic species such CrO_4^{2-} , HCrO_4^- or $\text{Cr}_2\text{O}_7^{2-}$ that do not tend to form insoluble salts with Ca(II) ions. The adsorption of PO_4^{3-} was higher than that of SO_4^{2-} in agreement with the lower solubility of $\text{Ca}_3(\text{PO}_4)_2$ compared to CaSO_4 . The combined use of the nanostructured calcium silicate with Al(III) using poly-aluminium chloride improves the sulphate adsorption, even starting from initial solutions that contain over 2–5 g/L, obtaining a raffinate solution containing only a few mg/L accomplishing this way with the Chilean environmental regulations of discharge. The formation of ettringite, a double calcium and aluminium basic salt, during the adsorption would explain these results. Then, it is possible to achieve an almost complete sulphate removal.

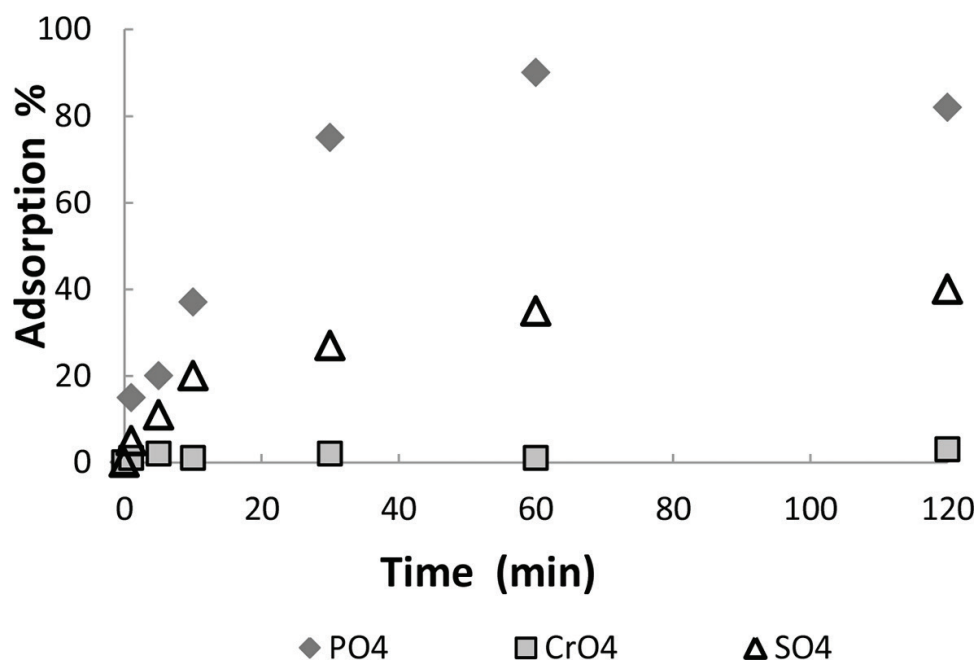


Figure 5. Adsorption of some anionic species onto nanostructured calcium silicate.

The dissolved species diffuse from the solution to the surface of the adsorbent, and then to the internal structure. The rate of adsorption is usually limited by mass transfer and depends on the properties of the sorbate and sorbent. The equilibrium adsorption results of ionic species adsorption have been explained using conventional equilibrium isotherms including the Langmuir model, the empirical Freundlich model and the Redlich-Peterson isotherm, which is a hybrid sorption model employed to analyse experimental data that do not fit well with other mentioned models. Normally, Langmuir isotherm only can explain the experimental results when synthetic and quite pure and ideal aqueous solutions are used. Freundlich and Redlich-Peterson used to fit equilibrium experimental results when real mining or more complex chemical matrices are used as aqueous solutions. With respect to kinetics experiments, normally experimental results are satisfactorily well explained by applying a pseudo-second-order kinetics model which is based on the sorption capacity of the sorbent.

2.7. Conclusions

In general, the modification with other atoms like Fe, Al and Mg of the nanostructured calcium silicate hydrate does not affect its high potential as adsorbent for treating polluted acidic solutions. The modified materials are superior to the unmodified material in terms of stability and sorption capacity by forming highly insoluble and stable double salts. The silicates would act as seeding material of insoluble hydroxides and salt species.

3. Natural sorbents case study: biosorbents - pine bark

3.1. Introduction

Several natural and low-cost products have been assessed as sorbents or as removal agents for heavy metal ions and other pollutants present in industry-discarded aqueous solutions [22–25]. Some examples of biosorbents are sugar maple [26]; mulch [27]; papaya wood [28]; tea industry wastes [29]; sawdust [30] and pine bark [31]. Particularly, the primary use of bark (and other by-products of the wood industry) is mainly associated with fuel with little added value. Therefore, their use as a sorbent is expected to produce an increase of the overall industry sustainability. Moreover, its use as biosorbent may become especially interesting when the pollutant loaded material can undertake further steps leading to its reutilisation as a sorbent (elution, pyrolysis, etc.) or carry on with other uses such as the production of activated carbon.

In this case, the adsorption efficiency, evaluated in terms of the adsorption capacity, varies from only a few micrograms up to 200 mg per grams of dry bark. The efficiency of the overall wastewater treatment process depends on the type of natural sorbent, the nature of the metal or pollutant to be adsorbed, the initial pollutant concentration, pH, temperature, pulp density, the cell design (batch, column, etc.) and the contacting time. In fact, many scientific reports have revealed that this material can adsorb and act simultaneously as biofilter for several types of pollutants, such as heavy metals and organic products.

This chapter focuses on the treatment of wastewaters containing heavy metals commonly observed at large scale operations related to industrial activities such as mining and metallurgical processes [32, 33]. The use of adsorption techniques overcomes this problem leaving aqueous solutions with heavy metal concentrations typically in the order of parts per billion [28].

It has been shown that the governing mechanism for the adsorption of cationic heavy metals using biosorbents is based on ionic exchange reactions [34], which occurs throughout the removal of protons present in the different bark molecular structures (Eq. (13)),



where R represents the organic structure of the sorbent, M^{n+} is the dissolved heavy metal ion in solution. As a consequence of the adsorption, the acidity of the aqueous phase increases. The adsorption may coordinate one or more adsorption sites and the charge of the metallic ion can be totally or partially compensated by the surface charge of the biosorbent.

3.2. Substrate pre-treatment

One problem associated with the use of pine bark in the removal of heavy metals is its content of natural organic complexation agents such as tannins, which can be released in significant concentrations and stabilise contaminants in solution rather than removing them. There are a number of biosorbent pre-treatments reported in the literature aiming at removing or fixing such soluble compounds and simultaneously improving the subsequent pollutant adsorption efficiency/capacity. For instance, it has been shown that best adsorption results are obtained throughout carrying out a prior 'bark chemical activation'. This treatment consists of immersing the pine bark into diluted acid media at slightly high temperatures such as 50°C–70°C [34–36] before performing the adsorption tests. The acidic solution needs to be diluted to secure the integrity of the sorbent during the pre-treatment. The pH range in which the impact of chemical activation is the highest is narrow and it depends on the heavy metal nature and on the pulp density used [37]. Another pre-treatment consists of just washing the pine bark with water facilitating the removal of tannins and other soluble species which, if not removed, could again, irreversibly pollute even more the wastewater.

3.3. Experimental procedures

This experimental part gathers a number of findings concerning the bark structure, its response to chemical activation, and experiments generating adsorption equilibrium and kinetic data.

3.3.1. Pine bark characterisation and preparation

Pine bark samples are reduced in size to particle size distributions below 1 mm diameter (16# Tyler). The chemical activation is commonly performed using sulphuric acid 0.1–0.2 M and up to 1 M for 2 h at a temperature ranging from 20°C to 50°C with a solid to liquid ratio equal to 1:10.

Pine bark washing procedures are carried out with distilled water in a Soxhlet apparatus. Scanning electron microscopy (FEI Quanta 250 FEG SEM) is used to analyse the pine bark unloaded and loaded with the pollutant. Semi-quantitative elemental analysis was performed by EDX analysis of fluorescence intensities. FT-IR spectroscopy experiments are carried out on an IFS 55 spectrometer (Bruker) using diffuse reflectance mode (Harrick Attachment). The detector was of an MCT type and cooled at liquid nitrogen temperature (77 K).

XPS analysis is performed using a Kratos Axis Ultra instrument with a monochromatic Al K_{α} source. Samples are fixed on the sample holder using double-sided tape.

3.3.2. Adsorption studies

In all cases, there is an initial concentration of the pollutant (heavy metal) commonly in the dissolved state in the aqueous phase and introduced as a sulphate or a nitrate salt. The pH condition is close to the point where the hydrolysis starts producing insoluble or neutral species. All tests are carried out at 20°C and the pulp density used varies from 1 to 20 g sorbent/L.

aqueous solution unless stated otherwise. The adsorbed amount of pollutant is obtained by computing the difference between the initial amount of pollutant and the residual concentration after adsorption. The metal concentration in solution is obtained using atomic absorption spectrophotometry (AAS) Perkin Elmer Model 2380.

Equilibrium data are obtained at least after 48 h contact between the sorbent and the polluted aqueous phase. Kinetic data are generated following similar experimental protocols

In all cases, high purity reagents were used. Further details or changes in this procedure are pointed out when appropriate.

3.4. Results

3.4.1. Characterisation and modelling of the substrate

Table 3 shows the chemical composition of both raw and chemically (acid) activated bark resulting from the EDX elemental analysis of original washed bark and after the sulphuric acid treatment. As expected, most of the soluble species decrease their content due to the activation. The acid treatment reduces the concentrations of K, Mg, Mn and Ca significantly, whereas other metal concentrations (Na, Al, Si, Ti, Fe, Cu) remain almost constant.

Bark	Chemical element									
	Na	K	Mg	Ca	Al	Si	Ti	Mn	Fe	Cu
Washed	0.98	2.03	2.40	12.80	6.40	17.10	0.47	0.57	4.80	0.025
Activated	0.94	1.08	0.79	5.70	7.00	21.30	0.46	0.11	4.30	0.025

Table 3. Semi-quantitative EDX analysis of pine bark (values are in mg per g of dry bark).

Figure 6 shows the DRIFT analysis obtained for a section of the finger print region. A broad band is observed from 3600 to 3000 cm^{-1} , indicating the presence of O-H and C-H stretching vibrations. Between 2000 and 1500 cm^{-1} there is a strong band at 1610 cm^{-1} representing the carbonyl C = O stretch. When Pb(II) is adsorbed onto bark, a broadening of the band occurs and a simultaneous modifications at wavenumbers of approximately 1512 cm^{-1} related to aromatic skeletal vibrations. These changes are in agreement with the structures which are easier to ionise (**Figure 7**).

A high concentration of the metallic ions in solution may then activate the adsorption sites having lower ionization constant ultimately increasing the specific adsorption.

Figure 8 shows the SEM images after sorption using low pulp densities conditions. EDX elemental analysis at the spots vmarked in the figures revealed a high heterogeneity in the Pb distribution across the bark. The Pb/O weight ratio varied from 2:1 to 3:1 regardless the pulp density value. Similar observations of varying metal content were previously seen for untreated bark [39].

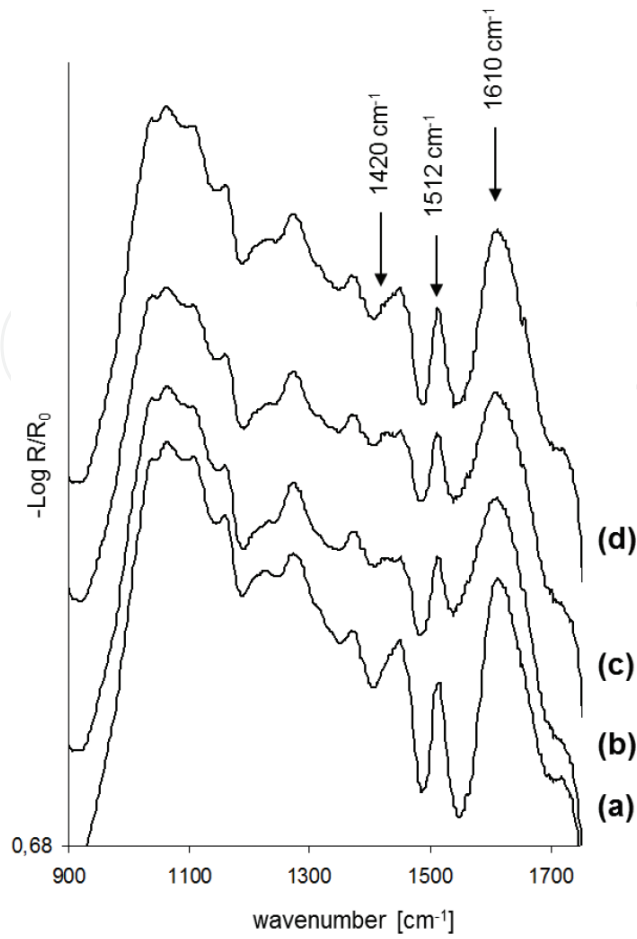


Figure 6. DRIFTS spectra for activated bark (a) and bark charged with solutions containing 1 (b), 1.5 (c) and 3 (d) g Pb L⁻¹. Pulp density: 1.5 g/L.

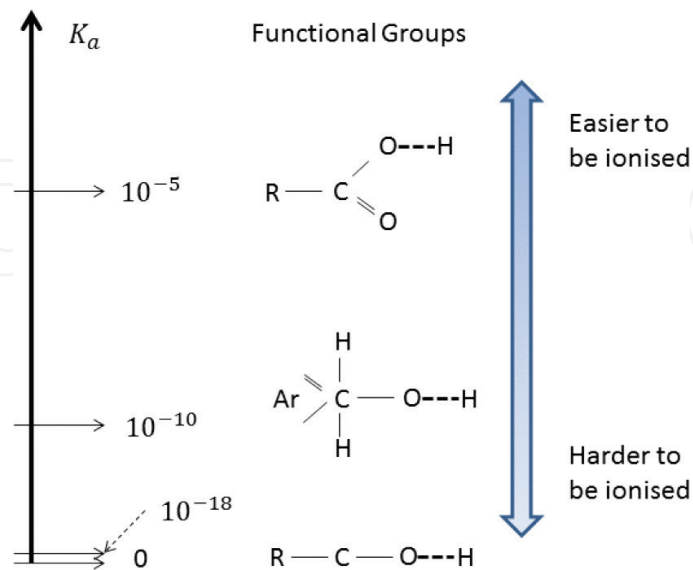


Figure 7. Schematics of the organic groups, its relative proportion in the structure of bark, and radicals through which the ionization could lead to heavy metals adsorption onto bark. K_a represents the acidity constant, C: carbon, O: oxygen, Ar: aromatic structure (from Ref. [38]).

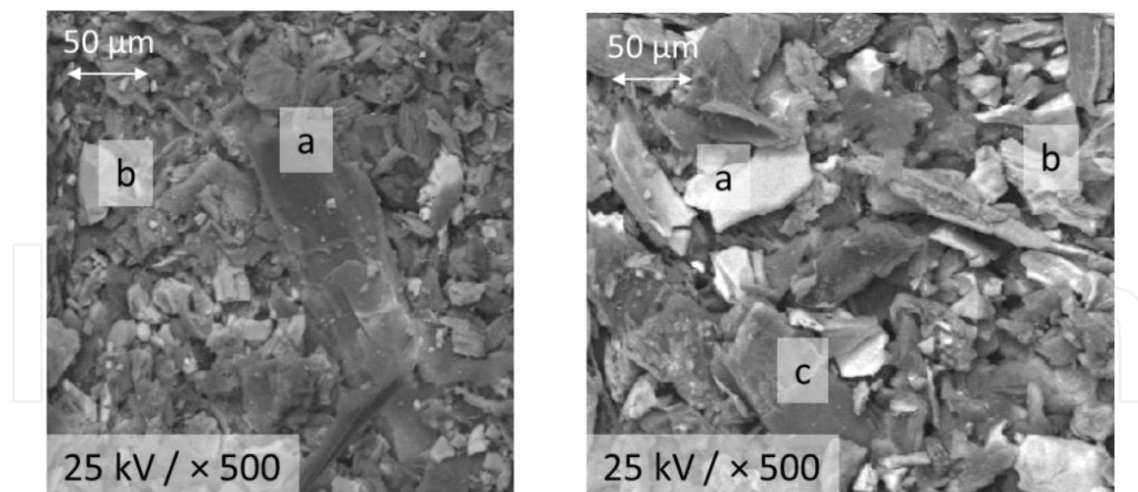


Figure 8. SEM images of activated pine bark loaded with adsorbed Pb(II). Left: pulp density 1.0 g/L. EDX analysis indicates Pb/O weight ratios of 2:1 and 3:1 in spots (a) and (b), respectively. Right: pulp density 1.5 g/L. EDX indicates Pb/O weight ratios decreasing from (a) to (c) ranging from approximately 2:1 to 3:1.

3.4.2. Adsorption tests: thermodynamics and kinetics

As an example, **Figure 9** shows the adsorption percentage of Cu(II) from batch experiments. Langmuir and Freundlich isotherms fit well with the experimental data. The adsorption capacity varies from one chemical element to another and as a function of the experimental conditions used. Pb(II) ions reach similar adsorption capacity at 10 g/L pulp density but it can reach 90 mg/g at 1 g/L. Concerning adsorption competitive reactions, when comparing Cu(II) and Zn(II) adsorption, Cu(II) reaches higher adsorption capacities than Zn(II). Binary adsorption reveals both metallic ions which do not interfere in the adsorption of each other reaching similar adsorption capacities when mixed and separated; however, this is not the case for all metals. Al-Asheh and Duvnjak (1997) have proved that Ni^{2+} and Cu^{2+} interfere slightly whereas the pairs $(\text{Cu}^{2+}, \text{Cd}^{2+})$ and $(\text{Cd}^{2+}, \text{Ni}^{2+})$ show a more significant interaction [22].

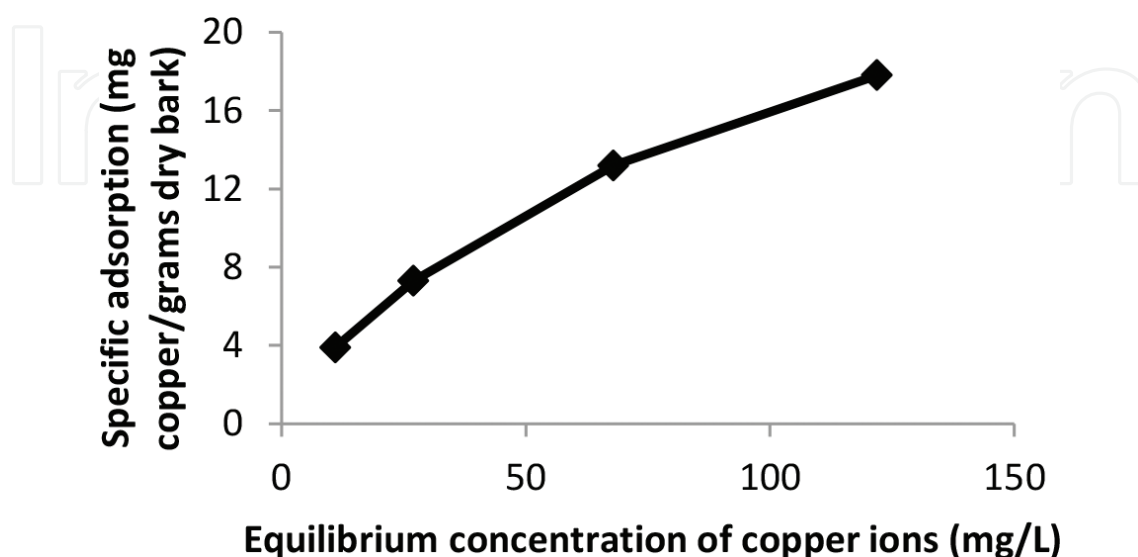


Figure 9. Adsorption isotherm of copper (II) ions onto washed pine bark at pH 5, 10 g/L pulp density [40].

If the heavy metal needs to be recovered, elution stages may allow removing and concentrating at least 90 and 71% or Cu(II) and Zn(II), respectively. The resulting solutions are 20 and 9 times more concentrated than the original polluted solution [41]. In consequence, the zinc surface complexes are more stable than the ones of copper. **Figure 10** shows the adsorption percentage and the specific adsorption results of copper obtained at different pulp densities with washed and activated pine bark.

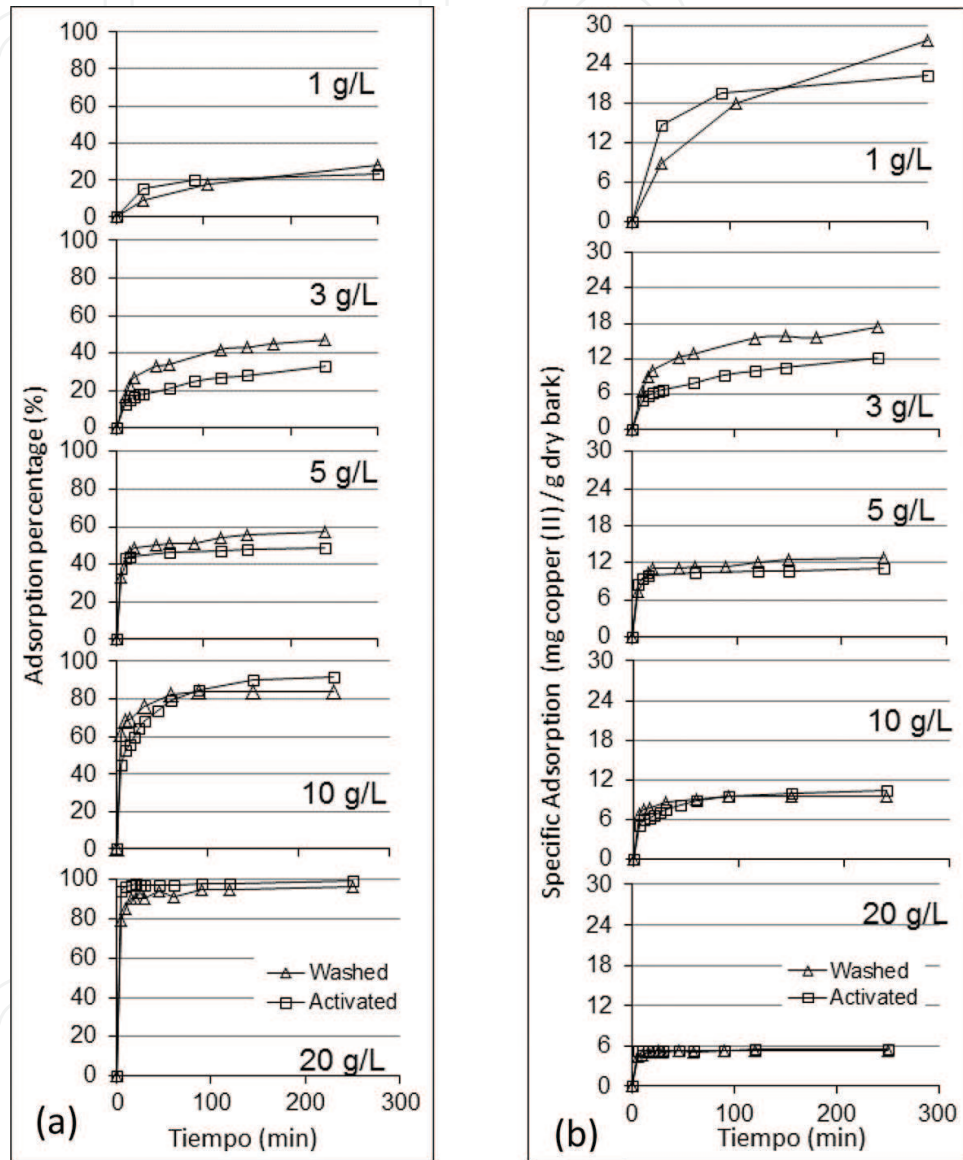


Figure 10. (a) Kinetics of adsorption percentage (%) and (b) specific adsorption (mg copper (II) ions/g dry bark) of copper (II) ions onto washed and activated bark [42].

The higher the pulp density (number of sorbent surface sites available), the higher the amount of metal removed from solution. Depending on the pulp density, the concentration of the heavy metal in solution and the contact time of the solution with the bark, the adsorption percentage may reach a *plateau* or maximum value. Such maximum value is usually referred to as 'saturation' which might be misleading. It can also be observed that the higher the pulp

density, the lower the specific adsorption. At constant initial metal concentration, the increase of pulp density favours the adsorption process on bark surface sites that are easier to reach and to be replaced by a metal ion (high energy surface sites). In other words, the material is not being used at its maximum capacity.

Moving from the high to low pulp density values, the specific adsorption increases. This indicates that higher concentrations of copper (II) ions activate sites. This is expected, given that the increase of copper (II) ions will shift the adsorption equilibrium constants of secondary reactions towards increasing the metal concentration in its adsorbed state. Indeed, the ion exchange mechanism (the main responsible for metal adsorption) occurs throughout many organic radicals with different acidity constants.

3.4.3. Surface analysis of the sorbent

Several scientific reports have been devoted only to analyse and to interpret the results from X-ray photoelectron spectra of wood and compounds derived from it [43, 44]. **Figure 11** shows the O1s emission lines obtained for the untreated sample of pine bark and charged with Pb(II) ions. The energy scale was fixed and referred to 285 eV, in agreement with most studies reported [44].

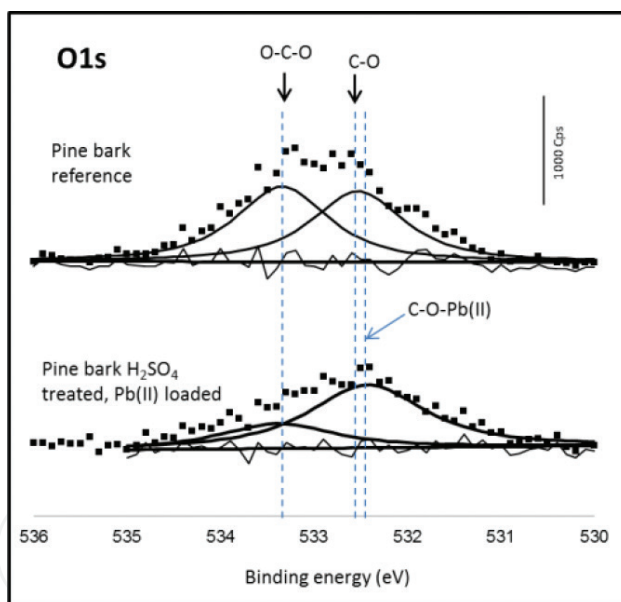


Figure 11. XPS spectra of pine bark samples. Sample 1: **Original** pine bark; sample 2 loaded for 24 h with Pb(II) in an acid aqueous solution (pH 5) at 5 g/L pulp density [45].

The O1s line is strongly perturbed by Pb(II) adsorption. The peak at the lowest position shifts to lower binding energy values, confirming a reductive environment due to Pb(II) adsorption. The peak associated with O-C-O is similarly shifted towards lower binding energies but in smaller magnitude compared to that representing C-O- type structures. Additionally, the intensity of C-O peak increases relative to the other peak. This suggests that not all sites present similar active sites. Most of them have C-O sites for adsorption while the amount of phenolic sites varies locally through bark structure. The mechanism, therefore, should take

place in well distributed C-O groups and as a second type of sites in significance it would be the phenolic groups. The latter is in agreement with DRIFT results.

3.5. Conclusions

Results have shown that the adsorption efficiency depends not only on the pollutant nature but also on the presence of other species which may interact with the pollutant interfering positively or negatively on the adsorption performance. There are cases where the simultaneous presence of different pollutants results in influencing the overall adsorption capacity (for example Cd(II) and other divalent ions) and other cases where pollutants adsorb regardless the presence of others (for example Cu(II) and Zn(II)). The elution process carried out with 1N nitric acid solution proved to be promising to concentrate both ions. Cu(II) ions were more likely to be destabilised than Zn(II). The tests performed with a pulp density of 6 mg/g dry bark resulted in solutions 20 and 9 times more concentrated in the case of Cu(II) and Zn(II), respectively. The chemical activation of pine bark material increases the rate at which copper (II) ions are adsorbed and it simultaneously reduces the maximum achievable adsorption equilibrium. The chemical activation is useful primarily at high pulp density values (above 10 g/L). The adsorption capacity for Pb(II) at very low pulp density is about 93.7 mg Pb(II)/g dry bark. Mono-hydroxylated species and free lead ions were presented as the major responsible for adsorption. DRIFTS analysis revealed that the adsorption mechanism is complex, mainly driven by bark surface sites involving C-O groups and this was confirmed by XPS analysis. Phenolic and cellulose oxygen sites are also relevant.

Acknowledgements

The authors wish to thank The National Fund for Development of Science and Technology of Chile, FONDECYT, for all the financial support throughout the Grant N° 1140331. The authors would like to dedicate this manuscript to Professor Sergio Montes Sotomayor for all his contributions to the field of wastewater treatment. We thank Mrs. Ana Maria Rojo MSc. for all her comments that greatly improved the manuscript.

Author details

Gonzalo Montes-Atenas^{1,*} and Fernando Valenzuela²

*Address all correspondence to: gmontes@ing.uchile.cl

1 Minerals and Metals Characterisation and Separation (M²CS) Research Group, Departamento de Ingeniería de Minas, Facultad de Ciencias Físicas y Matemáticas, Universidad de Chile, Santiago, Chile

2 Laboratorio de Operaciones Unitarias e Hidrometalurgia, Facultad de Ciencias Químicas y Farmacéuticas, Universidad de Chile, Independencia, Santiago, Chile

References

- [1] Johnson D., Hallberg K., Acid mine drainage remediation options: a review, *Sci. Total Environment*. 2005; 338: 3–14. DOI 10.1016/j.scitotenv.2004.09.002
- [2] Ziemkiewicz P., Skousen J., Brant D., Sterner P., Lovett R., Acid mine drainage treatment with armoured-limestone in open limestone channels, *Journal of Environmental Quality*. 1997; 26: 1017–1024. DOI: 10.2134/jeq1997.00472425002600040013x
- [3] Norm, D.S. MOP N° 601/2004, Maximum allowable limits for discharge of liquid wastes to continental and marine surface waters, Chile Government.
- [4] Hubbard C., Black S., Coleman M., Aqueous geochemistry and oxygen isotope compositions of acid mine drainage from the Río Tinto, SW Spain, highlight inconsistencies in current models, *Chemical Geology*. 2009; 265: 321–334. DOI: 10.1016/j.chemgeo.2009.04.009
- [5] Wisskirchen C., Dold B., Friese K., Spangenberg J., Morgenstern P., Glaesser W., Geochemistry of highly acidic mine water disposal into a natural lake with carbonate bedrock, *Applied Geochemistry*. 2010; 25: 1107–1119. DOI: 10.1016/j.apgeochem.2010.04.015
- [6] Valenzuela F., Cabrera J., Basualto C., Sapag J., Separation of zinc ions from an acidic mine drainage using a stirred transfer cell-type emulsion liquid membrane contactor, *Separation Science and Technology*. 2007; 42: 363–377. DOI: 10.1080/01496390601069887
- [7] Kalin M., Fyson A., Wheeler W., The chemistry of conventional and alternative treatment systems for the neutralization of acid mine drainage, *Science of the Total Environment*. 2006; 366: 395–408. DOI: 10.1016/j.scitotenv.2005.11.015.
- [8] Martell A.E., Hancock R.D. Metal Complexes in Aqueous Solutions. 1st ed. 1996 Springer Science+Business Media New York, Plenum Press, New York, US. 253 p. DOI: 10.1007/978-1-4899-1486-6
- [9] Defay R. and Prigogine I. Surface tension and adsorption (Treaty of Thermodynamics according to the methods of Gibbs and De Donder, Volume III, Tome III), Desoer Dunod Edition, 1951. 295 p. ISBN: 0582462843 9780582462847
- [10] Langmuir I., The adsorption of gases on plane surfaces of glass, mica, and platinum, *Journal of American Chemical Society*. 1918; 40: 1361–1403 DOI: 10.1021/ja02242a004
- [11] Brunauer S., The adsorption of gases and vapours. Princeton, USA: Princeton University Press, 1945, 528 p.
- [12] Freundlich, H.M.F. Concerning adsorption in solutions. *Zeitschrift für Physikalische Chemie-Stoichiometrie und Verwandtschaftslehre*, 1906, 57: 385–470. ISSN: 2196-7156
- [13] Redlich O., Peterson D.L., A useful adsorption isotherm, *Journal of Physical Chemistry*. 1958; 63: 1024–1024 DOI: 10.1021/j150576a611

- [14] Lagergren S. About the theory of so-called adsorption of soluble substances. 1898, *Kungliga Svenska Vetenskapsakademiens. Handlingar*. 1898; 24: 1-39. DOI: 10.1007/bf01501332
- [15] Weber W.J.Jr, Morris J.C., Kinetics of adsorption on carbón from solution, *Journal of Sanitary Engineering Division of the American Society of Civil Engineers*. 1963; 89: 31–60. DOI:
- [16] Valenzuela F., Basualto C., Sapag J., Ide V., Luis N., Narváez N., Yañez S., Borrmann T., Adsorption of pollutant ions from residual aqueous solutions onto nano-structured calcium silicate, *Journal of Chilean Chemical Society*. 2013; 58: 1744–1749. DOI: 10.4067/S0717-97072013000200023
- [17] Chen R, Tanaka H, Kawamoto T, Asai M, Fukushima C, Na H, Kurihara M, Watanabe M, Arisaka M, Nankawa T, Selective removal of cesium ions from wastewater using copper hexacyanoferrate nanofilms in an electrochemical system, *Electrochimica Acta*. 2013; 87: 119–125. DOI:10.1016/j.electacta.2012.08.124
- [18] Sirés I., Brillas E., Remediation of water pollution caused by pharmaceutical residues based on electrochemical separation and degradation technologies: a review, *Environment International*. 2012; 40: 212–229. DOI: 10.1016/j.envint.2011.07.012.
- [19] Cairns M, Borrmann T, Höll W, Johnston J, A study of the uptake of copper ions by nano-structured calcium silicate, *Microporous and Mesoporous Materials*. 2006; 95: 126–134. DOI: 10.1016/j.micromeso.2006.05.009
- [20] Qian Q, Chen Q, Machida M, Tatsumoto H, Mochidzuki K, Sakoda A, Removal of organic contaminants from aqueous solution by cattle manure compost (CMC) derived activated carbons, *Applied Surface Science*. 2009; 255: 6107–6114. DOI: 10.1016/j.apsusc.2009.01.060
- [21] Güell R, Fontàs C, Anticó E, Salvadó V, Crespo J, Velizarov S, Transport and separation of arsenate and arsenite from aqueous media by supported liquid and anion-exchange membranes, *Separation and Purification Technology*. 2011; 80:428. DOI: 10.1016/j.seppur.2011.05.015
- [22] Al-Asheh S, Duvnjak Z, Sorption of cadmium and other heavy metals by pine bark, *Journal of Hazardous Material*. 1997; 56: 35–51. DOI: 10.1016/S0304-3894(97)00040-X
- [23] Tiwari D, Mishra SP, Mishra M, Dubey RS, Biosorptive behaviour of mango and neem bark for Hg⁺², Cr⁺³ and Cd⁺² toxic ions from aqueous solutions: a radiotracer study, *Applied Radiation and Isotopes*. 1999; 50: 631–642. DOI: 10.1016/S0969-8043(98)00104-3
- [24] Vazquez G, Antorrena G, Gonzalez J, Doval MD, Adsorption of heavy metal ions by chemically modified Pinus pinaster Bark, *Bioresource Technology*. 1994; 48:251–255. DOI: 10.1016/0960-8524(94)90154-6
- [25] Martin-Lara MA, Blazquez G, Ronda A, Pérez A, Calero M, Development and characterisation of biosorbents to remove heavy metals from aqueous solutions by chemical treatment of Olive Stone, *Industrial and Engineering Chemistry Research*. 2013; 52:10809–10819. DOI: 10.1021/ie401246c

- [26] Watmough SA, Hutchinson TC Uptake of ^{207}Pb and ^{111}Cd through bark of mature sugar maple, white ash and white pine: a field experiment, *Environmental Pollution*. 2003; 121:39–48. DOI: 10.1016/S0269-7491(02)00208-7
- [27] Jang A, Seo Y, Bishop PL, The removal of heavy metals in urban runoff by sorption of mulch, *Environmental Pollution*. 2005; 133:117–127. DOI: 10.1016/j.envpol.2004.05.020
- [28] Saeed A, Akhter MW, Iqbal M Removal and recovery of heavy metals from aqueous solution using papaya wood as a new biosorbent, *Separation and Purification Technology*. 2005; 45:25–31. DOI: 10.1016/j.seppur.2005.02.004
- [29] Cay S, Uyanik A, Ozasik A, Single and binary component adsorption of copper(II) and cadmium(II) from aqueous solution using tea-industry waste, *Separation and Purification Technology*. 2004; 38:273–280 DOI: 10.1016/j.seppur.2003.12.003
- [30] Taty-Costodes VC, Fauduer H, Porte C, Delacroix A, Removal of Cd(II) and Pb(II) ions from aqueous solutions, by adsorption onto sawdust of *Pinus sylvestris*, *Journal of Hazardous Material*. 2003; 105:121–142 DOI: 10.1016/j.jhazmat.2003.07.009
- [31] Khokhotva AP, Adsorption of heavy metals by a sorbent based on pine bark, *Journal of Water Chemistry and Technology*. 2010; 32: 336–339. DOI: 10.3103/S1063455X10060044
- [32] Martins M, Faleiro ML, Barros RJ, Verissimo AR, Barreiros MA, Costa MC Characterization and activity studies of highly heavy metal resistant sulphate-reducing bacteria to be used in acid mine drainage decontamination, *Journal of Hazardous Material*. 2009; 166:706–713. DOI: 10.1016/j.jhazmat.2008.11.088
- [33] Huang S-C, Chang F-C, Lo S-L, Lee M-Y, Wang C-F, Lin J-D, Production of lightweight aggregates from mining residues, heavy metal sludge, and incinerator fly ash, *Journal of Hazardous Material*. 2007; 144:52–58 DOI: 10.1016/j.jhazmat.2006.09.094
- [34] Martin-Dupont F, Gloagen V, Guilloton M, Granet R, Krausz P, Study of chemical interaction between barks and heavy metal cations in the adsorption process, *Journal of Environmental Science Health, Part A*. 2006; 41:149–160. DOI: 10.1080/10934520500349250
- [35] Al-Asheh S, Banat F, Al-Omari R, Duvnjak Z, Predictions of binary sorption isotherms for the sorption of heavy metals by pine bark using single isotherm data, *Chemosphere*. 2000; 41:659–665. DOI: 10.1016/S0045-6535(99)00497-X
- [36] Teles de Vasconcelos LA, Gonzalez Beca CG, Chemical activation of pine bark to improve its adsorption capacity of heavy metal ions. Part 2: by conversion to a salt form, *European Water Pollution Control: Official Publication of the European Water Pollution Control Association (EWPCA)* 1997; 7:47–55. ISSN: 0925-5060
- [37] Celik A, Demirbas A, Removal of heavy metal ions from aqueous solutions via adsorption onto modified lignin from pulping wastes, *Energy Source*. 2005; 27:1167–1177. DOI: 10.1080/00908310490479583

- [38] Brown WH, Foote CS, Iverson BL, Anslyn E, Organic chemistry, 5 edition. 20 Davis Drive, Belmont, CA: Brooks Cole Cengage Learning, United States of America 2009, 1312 p. ISBN-10: 084005498X
- [39] Montes S, Montes-Atenas G, Vilches A, Study of removing copper (II) and chromium (VI) from aqueous solution using bark pine. Proceedings of the TMS Fall 2002 Extraction and Processing Division Meeting; September 2002. Lulea, Sweden: pp. 1–5.
- [40] Montes S, Montes-Atenas G, Salomo F, Valero E, Diaz O, On the adsorption mechanisms of copper ions over modified biomass, *Bulletin of Environmental Contamination and Toxicology*. 2006; 76: 171–178. DOI: 10.1007/s00128-005-0904-8
- [41] Montes S, Montes-Atenas G, García-García F, Valenzuela M, Valero E, Díaz O, Evaluation of an adsorption-desorption process for concentrating heavy metal ions from acidic wastewaters, *Adsorption Science and Technology*, 2009; 27: 513–521. DOI: 10.1260/0263-6174.27.5.513
- [42] Montes-Atenas G, Valenzuela F, Montes S, The application of diffusion-reaction mixed model to assess the best experimental conditions for bark chemical activation to improve copper(II) ions adsorption, *Environmental Earth Sciences*. 2014, 72: 1625–1631. DOI: 10.1007/s12665-014-3066-3
- [43] Nzokou P, Kamdem DP, You have free access to this content X-ray photoelectron spectroscopy study of red oak-(*Quercus rubra*), black cherry- (*Prunus serotina*) and red pine- (*Pinus resinosa*) extracted wood surfaces, *Surface and Interface Analysis*, 2005; 37: 689–694. DOI: 10.1002/sia.2064
- [44] Shchukarev A, Sundberg B, Mellerowicz E, Persson P, XPS study of living tree, *Surface and Interface analysis*. 2002; 34: 284–288. DOI: 10.1002/sia.1301
- [45] Montes-Atenas G, Schroeder SLM, Sustainable natural adsorbents for heavy metal removal from wastewater: lead sorption on pine bark (*Pinus radiata* D.Don). *Surface and Interface Analysis*. 2015; 47: 996–1000. DOI: 10.1002/sia.5807

IntechOpen